Original Article

DOI: 10.7860/JCDR/2023/58770.18016

Radiology Section

Utility of Contrast-enhanced 3D T1-weighted CUBE Fat Sat Sequence MRI to Evaluate Pathological Cranial Nerve Enhancement: A Cross-sectional Study

RUCHI GUPTA[1], AISHWERYA SINGH[2], MANISHA KUMARI[3], SANJAY KUMAR SUMAN[4], NEETU SINHA[5]

ABSTRACT

Introduction: Abnormal Cranial Nerve (CN) enhancement can point towards an underlying disorder or disease severity. Therefore, the depiction of this feature is of utmost importance in the evaluation of various pathologies. Various Magnetic Resonance Imaging (MRI) sequences have a role in the early identification of such findings.

Aim: To study the spectrum of cases of abnormal CN enhancement on MRI and the role of contrast-enhanced 3 Dimensional (3D) T1-weighted CUBE Fat saturated sequence in evaluating pathological CN enhancement.

Materials and Methods: This cross-sectional study was conducted in the Department of Radiodiagnosis at Indira Gandhi Institute of Medical Sciences, Patna, Bihar, India. The duration of the study was two years, from June 2020 to June 2022. Study included 50 patients who presented with signs and symptoms of CN involvement or were referred for other pathologies with incidental detection of pathological nerve enhancement on 1.5 Tesla (T) MRI Scanner. The data was transferred to a Microsoft excel 2010 sheet and results were expressed in terms of frequency and percentages.

Results: The mean age of the study participants was 33.3±20.9 years. Male to female ratio was 28:22=1.27:1. Infections were the most common cause of abnormal CN enhancement 26 (52%) cases followed by demyelination 3 (6%) cases, haematological malignancy 4 (8%) cases, metastatic neural infiltration 5 (20%), primary neural tumours 4 (18%), Bell's palsy 1 (2%) case, Tolosa Hunt Syndrome (THS) 1 (2%) case and idiopathic polyneuritis cranialis 1 (2%) case.

Conclusion: Contrast-enhanced 3D T1 CUBE Fat Saturation (FS) sequence is excellent in depicting abnormal CN enhancement, especially the cisternal segments.

Keywords: 1.5 Tesla, 3 dimensional, Magnetic resonance imaging

INTRODUCTION

A total of 12 pairs of CN symmetrically originate from different parts of the brain, including the cerebrum (I, II CN), midbrain (III, IV CN), pons (V to VIII CN) and medulla (IX to XII CN) [1]. MRI is the best imaging modality to anatomically map the CN and their pathologies. It can also detect changes in enhancement patterns indicating underlying pathology when their size or thickness is normal [1]. The abnormal CN enhancement can be present in a variety of clinical conditions, which vary from infection to demyelination, granulomatous disorders, primary neural or brain tumours, and metastatic disease [2]. Subtle neural enhancement can be missed on routine postcontrast 2D spin echo sequences due to its non volumetric nature. Hence, depiction of CN on routine postcontrast images is difficult and can be frequently missed. In this regard, 3D T1 CUBE sequence scores over the 2D sequence as it enables us to pick even subtle enhancements, which at times may be the only sign of underlying disorder [2-4].

The T1 CUBE is a 3D Fast Spin Echo (FSE) sequence that uses variable flip angle and higher Echo Train Length (ETL) train length. It reduces the acquisition time and acquires 3D volumetric data that can be reformatted into any plane without partial volume effect. The volumetric data helps in early detection of subtle neural enhancements which can be easily compared to the opposite side [3]. There is also suppression of signal from small blood vessels by applying techniques like spatial Presaturation, double inversion recovery, and motion sensitising magnetisation preparation [4]. Hence, signals from blood vessels at the brain surface are reduced (black blood imaging) leading to better delineation of meningeal or other pathological enhancement [3,5]. However, grey white matter interface is poorly distinct in CUBE images. The aim of the present study was to study the role of contrast-enhanced 3D T1-weighted CUBE FS sequence in evaluating pathological CN enhancement.

MATERIALS AND METHODS

This cross-sectional study was conducted in the Department of Radiodiagnosis at Indira Gandhi Institute of Medical Sciences, Patna, Bihar, India. The duration of the study was two years, from June 2020 to June 2022. Institutional Ethics Committee approval (1525/IEC/IGIMS/2020) was obtained.

Inclusion criteria: The patients who presented with signs and symptoms of CN involvement or referred for other pathologies with incidental detection of pathological nerve enhancement were included in the study. For e.g., complaints of vision loss if 2nd CN involvement, drooping of eyelid in 3rd CN palsy, extraocular muscle palsy in CN 3rd, 4th, 6th palsy etc.

Exclusion criteria: The patients with claustrophobia, cardiac pacemaker, cochlear implant, other MRI non compatible metallic implants, metallic foreign body and reduced glomerular filtration rate were excluded from the study. As study included contrast imaging in each case, pregnant females were also excluded considering lack of adequate safety data.

Study Procedure

Analysis of data of pathological CN enhancement in 50 patients who were imaged on 1.5T MRI Scanner (OPTIMA 450w, General Electric, and United States) was done. Routine MRI brain sequences including T1, T2, Fluid-attenuated Inversion Recovery (FLAIR), Diffusion and Susceptibility Weighted sequences (DWI and SWI)

were acquired. In addition to these, contrast enhanced conventional 2D spin echo T1 FS in three planes and 3D T1 CUBE FS sequence in sagittal plane were also taken after injection of gadolinium-based MRI contrast (dose-0.1 mmol/kg body weight). The imaging parameters of 3D T1 CUBE sequence given in [Table/Fig-1].

Field of view (cm)	40×40
Matrix size	352×160
TR (ms)	640
TE (ms)	17
Flip angle	90
Slice thickness (mm)	1.2 mm
Number of excitations	0.55
Scan time (minutes)	3.15
Parallel imaging factor	2
Echo train length	28

[Table/Fig-1]: Imaging parameters for T1 CUBE FS sequence.
TR: Repetition time; TE: Time to Echo

STATISTICAL ANALYSIS

The data was transferred to a Microsoft excel 2010 sheet and results were expressed in terms of frequency and percentages.

RESULTS

The mean age of patients was 33.3±20.9 years. Male to female ratio was 28:22=1.27:1. Overall, the most common cause of abnormal CN enhancement N=26 (52%) cases in the study was infections with CNS tuberculosis being the most common. The various pathologies are summarised in the [Table/Fig-2] and the spectrum of various CN involvement and their associated pathologies are summarised in [Table/Fig-3].

S. No.	Aetiology	No. of patients (percentage)
1	CNS tuberculosis	17 (34%)
2	Fungal disease	4 (8%)
3	Viral disease (viral meningoencephalitis, herpes zoster ophthalmicus, viral labyrinthitis)	4 (8%)
4	Demyelination (isolated Optic Neuritis (ON), neuromyelitis optica syndrome, anti MOG antibody)	3 (6%)
5	Lyme's disease	1 (2%)
6	Bell's palsy	1 (2%)
7	Benign primary nerve tumour (acoustic schwannoma, optic glioma, trigeminal schwannoma)	6 (12%)
8	Malignant primary nerve tumour (bilateral retinoblastoma, gliomatosis cerebri with high-grade transformation, glioblastoma multiforme with meningeal carcinomatosis)	3 (6%)
9	Haematological malignancy (ALL, CLL, burkitt's lymphoma)	4 (8%)
10	Brain metastasis with neural infiltration (breast cancer)	2 (4%)
11	Perineural spread of tumour (from nasopharyngeal Ca, oropharyngeal Ca, maxillary Ca)	3 (6%)
12	Tolosa hunt syndrome	1 (2%)
13	Idiopathic polyneuritis cranialis	1 (2%)
Total		50

[Table/Fig-2]: Summarises various aetiologies seen in the patients.
CNS: Central nervous system; ALL: Acute lymphocytic leukaemia; CLL: Chronic lymphocytic leukaemia; Ca: Carcinoma; MOG: Myelin oligodendrocyte glycoprotein

[Table/Fig-4] illustrates normal CN anatomy on 3D T1 CUBE postcontrast MRI. In the present study, 17 patients were of CNS tuberculosis with 16 having multiple nerves involvement. The 3rd CN involvement was most common and seen in 15 (88%) cases. The 12th nerve was least commonly involved, seen in 1 (5.8%) case only [Table/Fig-5-7]. In cases, where optic nerve involvement was seen, perineural enhancement along the optic nerve and optic chiasma was the most common feature.

Cranial nerves	Cranial Nerve (CN) enhancement n (%)	Pathologies associated n (%)
1	None	None
2	21 (42%)	Infections-12 (57%), malignant nerve infiltration-3 (14%), primary neoplasm-2 (10%), demyelinating disorder-4 (19%)
3	25 (50%)	Infections-18 (72%), malignant nerve infiltration-5 (10%), tolosa hunt syndrome-1 (4%), idiopathic polyneuritis cranialis-1 (4%)
4	10 (20%)	Infections-7 (70%), malignant nerve infiltration-2 (20%), idiopathic polyneuritis cranialis-1 (10%)
5	30 (60%)	Infections 18 (60%), malignant nerve infiltration-9 (30%), primary nerve tumour-2 (6.6%), idiopathic polyneuritis cranialis-1 (3.3%)
6	11 (22%)	Infections-10 (91%), malignant nerve infiltration-1 (9%)
7,8	22 (44%)	Infections-12 (54%), Bells's palsy-1 (4.5%), Primary nerve tumour-4 (18%), malignant nerve infiltration-5 (23%)
9,10,11	10 (20%)	Infections-7 (70%), malignant nerve infiltration-2 (20%), idiopathic polyneuritis cranialis-1 (10%)
12	1 (2%)	Infection-1 (100%)

[Table/Fig-3]: Shows the spectrum of various Cranial Nerve (CN) involvement and their associated pathologies (N=50).

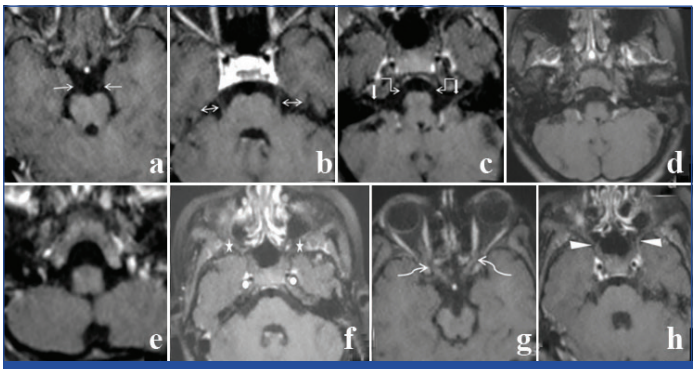

[Table/Fig-4]: Normal CN anatomy. (a-h) Axial reformatted T1 CUBE postcontrast images shows faintly seen bilateral 3rd nerves (white arrows), 5th (double headed arrows), 6th (curved white arrows), 7-8th nerve complex (block white arrows), bilateral pterygopalatine fossa (star), Meckel's cave (circle), optic nerve at orbital apex (curvilinear arrows) and maxillary nerves in foramen rotundum (arrow head).

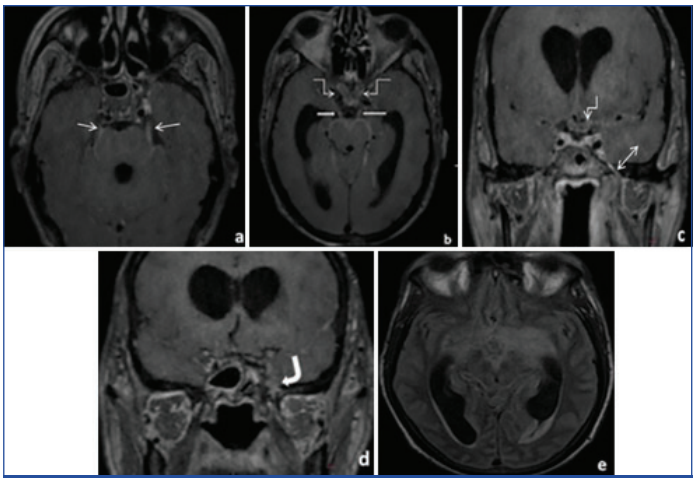

[Table/Fig-5]: Tubercular meningitis (TBM) with neuritis: A 40-year-old male presented with fever, altered sensorium and signs of raised intracranial tension. Postcontrast 3D T1 CUBE FS Axial (a,b) and Coronal (c,d) Reformatted images shows enhancing bilateral 5th nerves (white arrows), 3rd nerves (white block arrows), perineural enhancement of intracranial segment of optic nerves and optic chiasma (curved arrows), enhancing left V3 segment of trigeminal nerve in foramen ovale (double-headed arrow), left V2 segment in foramen rotundum (curved block arrow). Axial FLAIR image; (e) Shows Basal exudates and hydrocephalus with periventricular interstitial oedema.

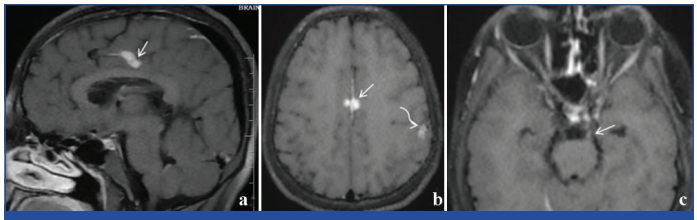

[Table/Fig-6]: Brain tuberculomas with neuritis: A 13-year-old female presented with headache, vomiting and left 3rd nerve palsy. Sagittal (a) and Axial (b) Postcontrast T1 CUBE FS images show two ring enhancing lesions in bilateral cingulate gyrus with thin dural enhancement (arrows). (b) Two conglomerate small ring enhancing lesions seen in left postcentral sulcus (curved arrow). (c) Subtle enhancement of left 3rd nerve seen (white arrow).

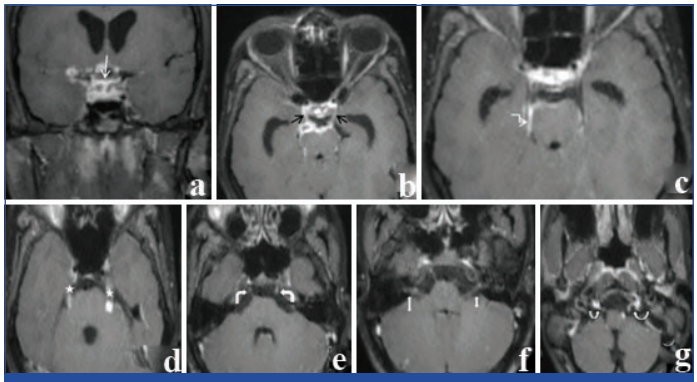

[Table/Fig-7]: CNS tuberculosis with neuritis. A 20-year-old male. Enhancement of (a) Optic chiasma (white arrow); (b) Bilateral 3rd (black arrows); (c) Right 4th nerve (curved arrow); (d) Bilateral 5th (star); (e) 6th (curved block arrows); (f) 7-8th (double-headed arrows); and (g) 9-10-11th nerve complex (thin curved block arrows) seen.

DISCUSSION

The CN are lined by connective tissue sheaths including endoneurium, perineurium, and epineurium. The tight junctions in the endothelium of endoneural capillaries and in the inner layers of perineurium, maintain the blood-nerve barrier and its disruption leads to leakage of contrast material resulting in perineural enhancement [2]. The geniculate, tympanic, and mastoid segments of the facial nerve may show enhancement due to the presence of perineural and epineural venous plexuses, however, the intracanalicular-labyrinthine segment does not normally enhance [2]. Similarly, trigeminal ganglion and proximal portion of its divisions do not normally enhance, however, surrounded by enhancing perineural vascular plexus. Enhancement of cisternal portion of the CN is always abnormal [6]. The various pathologies which can show abnormal CN enhancement include neoplasm, infections, inflammation, autoimmune, demyelinating, granulomatous, postradiation neuritis, infarction, brain contusion and primary nerve tumours [6-8].

Infections

Tuberculosis: CNS infections may result from variety of causes, like bacterial, viral, fungal or parasitic in aetiology [9]. CNS tuberculosis is still a challenging disease in many countries like India, where tuberculosis is endemic [10]. Clinical manifestations of pathological CN depend on the nerve involved. The presentation can be variable like visual loss, hearing impairment, loss of sensory or motor function in the nerve distribution and other signs of CN palsies. MRI is really helpful in diagnosing leptomeningeal enhancement, tuberculomas, brain abscesses, infarcts and hydrocephalus associated with CNS tuberculosis. Thick basal exudates in CNS tuberculosis may encase the optic chiasma and other CN in the cisterns, as well as, their roots [10]. A 3D TI CUBE postcontrast sequence helps in depicting abnormal CN enhancement in tuberculosis patients as complete cisternal course can be visualised due to 3D volumetric nature that may not be seen on routine conventional T1 spin echo postcontrast study. In a series of critically ill patients, spectrum of CNS infections was studied and it was found that, Tubercular Meningitis (TBM) was the commonest, followed by viral encephalitis, pyogenic and fungal meningitis in that order [9]. Li X et al., studied the CN palsies in TBM and found that, 3rd nerve palsy was the commonest (56.9%) followed by 2nd (52.8%), 6th (4.2%) and 8th nerve palsy (13.9%). A 25% of patients had more than one CN involvement [11]. The findings of the present study were quite similar to the study done by Li X et al.

Viral infection: Viral meningoencephalitis can also present with involvement of CN [Table/Fig-8]. Optic Neuritis (ON) and orbital apex syndrome, although rare, may be seen in herpes zoster ophthalmicus. Presence of unilateral optic nerve enhancement or trigeminal nerve complex in postcontrast study can also be seen. Enhancement can be best visualised in 3D TI CUBE sequence and thus, strengthen the diagnosis and support clinical findings of sensory or visual disturbance in patients with herpetic rash [Table/Fig-9,10].

Viral neuritis and labyrinthitis present with unilateral acute vertigo or hearing loss with associated nausea and vomiting. The cisternal segment of vestibular nerve or labyrinth appear hyperintense on T2 and FLAIR images and showed enhancement in postcontrast sequences, better appreciated in 3D T1 CUBE images [Table/Fig-11] [8].

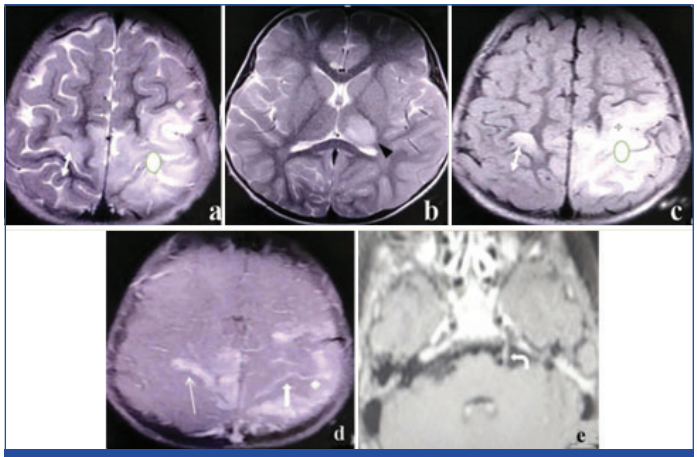

[Table/Fig-8]: Meningoencephalitis with left trigeminal neuritis: A 6-year-old female presented with history of high-grade fever and altered consciousness. (a,b) T2 weighted and (c) FLAIR axial images show gyral hyperintensity in right precentral gyrus (double-headed white arrow) and left high frontal and parietal region with perilesional oedema (white oval) and left thalamus hyperintensity (black arrow head in b). (d) A 2D T1 postcontrast axial image shows sulcal (white block arrow) and gyral pattern of enhancement (white arrow). (e) T1 CUBE post Gadolinium (GAD) axial reformatted image shows left trigeminal nerve enhancement (curved block arrow).

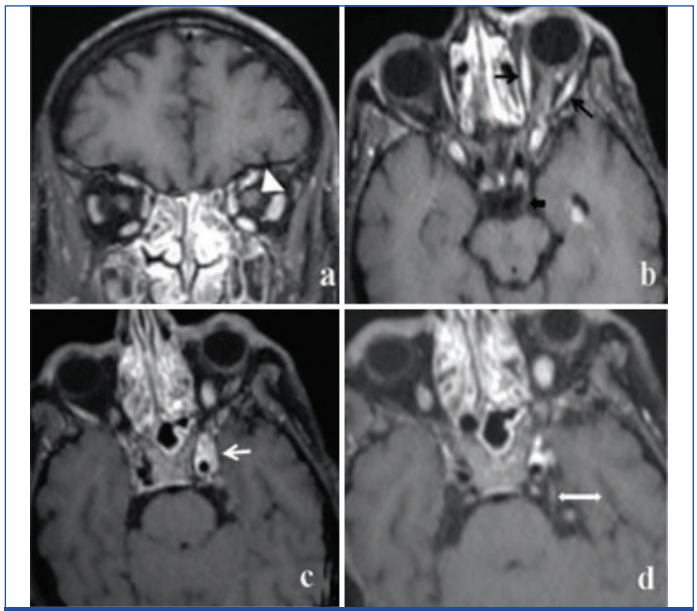

[Table/Fig-9]: Herpes zoster ophthalmicus. A 62-year-old male presented with resolving 3rd nerve palsy, multiple crusted lesions over left half of face and burning sensation. Postcontrast T1 CUBE sequence: (a) Shows enhancing and thick optic nerve (white arrow head); (b) Enhancing left extraocular muscles (black arrows) and left 3rd nerve (black block arrow); (c) Enhancing soft tissue in left cavernous sinus (white arrow); (d) Retrograde enhancement of left 5th nerve seen (double headed arrow).

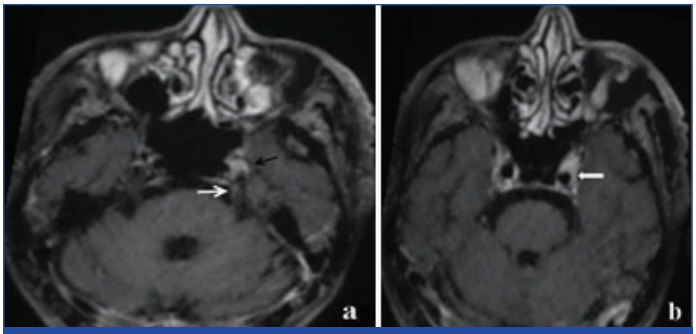

[Table/Fig-10]: Herpes zoster ophthalmicus. Known case of hypertension with vesicles over left half of face for 2-3 days and pain in left half of face for six days. Postcontrast T1 CUBE sequence with axial reformation shows: (a) Subtle enhancement along cisternal segment of left 5th nerve (white arrow), in Meckel's cave (black arrow); and (b) Enhancement in left cavernous sinus (block white arrow).

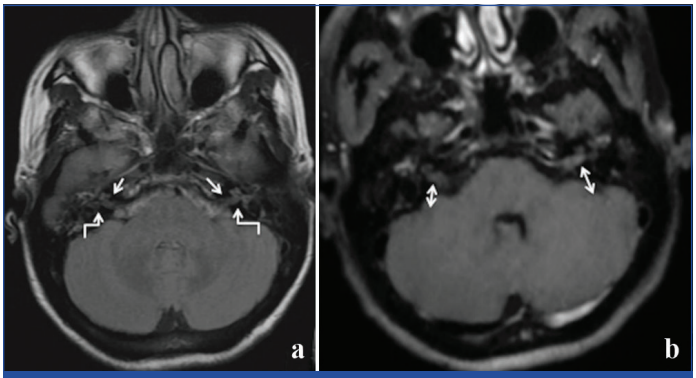

[Table/Fig-11]: Viral labrynthitis. A 45-year-old female presented with left-sided tinnitus and vertigo and fever for few days: (a) Axial FLAIR image shows hyperintense bilateral 7-8th nerve complex (white arrows), cochlea and semicircular canals (curved white arrows); (b) Postcontrast axial 3D CUBE T1 image shows enhancement of intracanalicular segment of bilateral 7-8th nerve complex, subtle enhancement of bilateral cochlea and semicircular canals also seen (double-headed arrows).

Fungal infection: Fungal infections of CNS can manifest as meningitis, cerebritis, abscess formation, cryptococcoma, and vasculitis depending upon the immune status of the patient [12]. Intracranial extension of disease from infected paranasal sinuses can lead to cavernous sinus thrombosis, involvement of the optic nerves with variable signs and symptoms. These findings are best evaluated by MRI and even subtle nerve enhancement can be picked up by post Gad 3D T1 black blood imaging [Table/Fig-12,13].

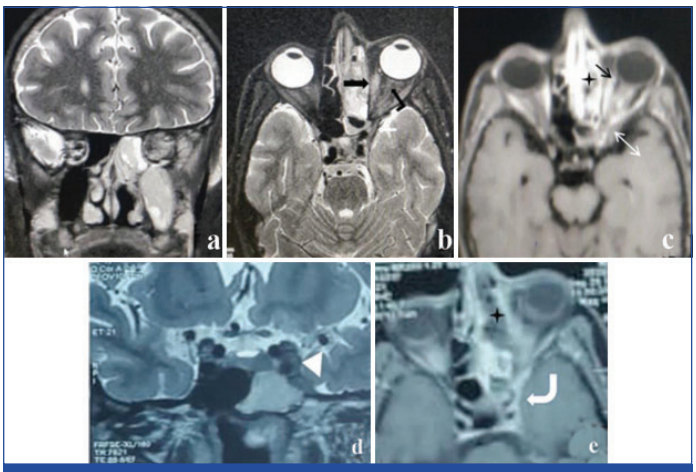

[Table/Fig-12]: Fungal sinusitis with orbital apex syndrome, cavernous sinus and dural extension. A 35-year-old male, known diabetic, presented with fever and nose bleed followed by complete ptosis and ophthalmoplegia and central retinal artery occlusion on left-side. T2 Coronal (a) and Axial (b) Left-sided pansinusitis and hyperintense left extraocular muscles (block black arrow) and optic nerve (curved black arrow). Mild T2 hypointense soft tissue seen at orbital apex (white block arrow) and along the left cavernous sinus and left medial temporal dura (white arrow head); (d) Postcontrast T1 CUBE reformatted axial image; (c,e) Shows peripherally enhancing sinus secretions to suggest active infection (black star), enhancing left extraocular muscles (black arrow), left orbital apex (white double-headed arrow), cavernous sinus and dura in medial temporal region (white curved arrow).

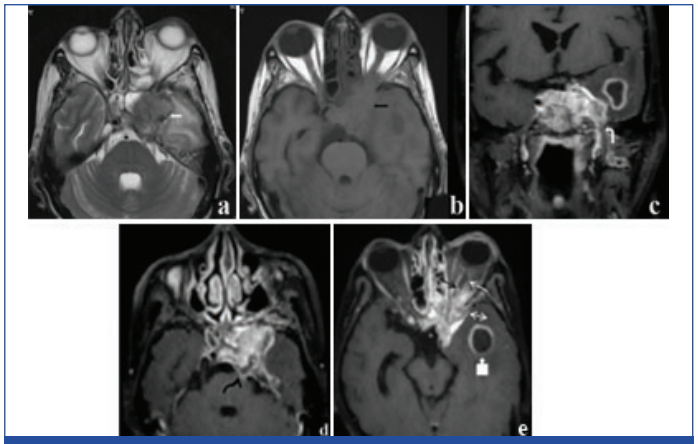

[Table/Fig-13]: Invasive fungal sinusitis. A 55-year-old male, diabetic, presented with loss of vision in left eye and left-side proptosis. (a) T2 hypointense (white block arrow) and (b) Mild T1 hyperintense lesion (black block arrow) seen in left sphenoid sinus with extension to right-side. (c) The lesion shows heterogenous moderate enhancement with abscess in left temporal lobe, extending into V3 branch of 5th nerve (curved white arrow); (d) Meckel's cave with retrograde involvement of 5th nerve upto pons (curved black arrow); (e) Left orbital apex (double-headed arrow), enhancement of optic nerve sheath (white arrow in e) and focal intrasubstance enhancement (black arrow) seen.

Lyme's disease: Lyme disease, also known as borreliosis, is caused by the bacteria Borrelia burgdorferi and the vector of the disease is ixodid tick [Table/Fig-14]. The disease may cause focal lesions in the white matter of brain, nerve root or meningeal enhancement and may affect other organ systems.

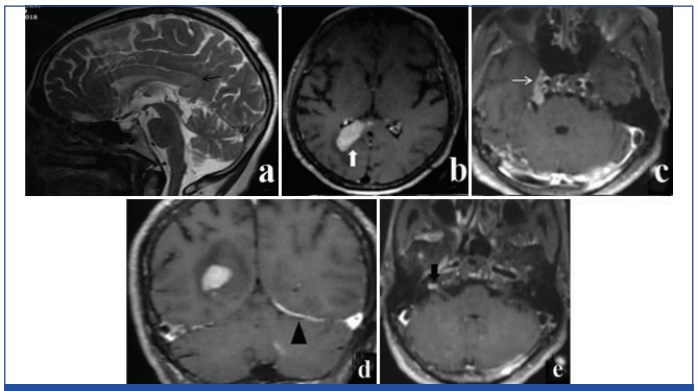

[Table/Fig-14]: Lyme's disease. A 55-year-old female presented with complaints of fever, headache for 15 days and altered sensorium for 3 days. Patient died after a day, further work-up couldn't be done. Sagittal T2 image: (a) Diffuse thickening with T2 hyperintensity within body and splenium of corpus callosum (black arrow), T1 CUBE FS postcontrast image; (b) Shows homogenous enhancement in right posterior periventricular and occipital white matter extending into splenium of corpus callosum (block white arrow); (c) Thickened enhancing right trigeminal nerve complex (white arrow); (d) Thickened enhancing left tentorium cerebelli (black arrow head); (e) Patchy enhancement in 7-8th nerve complex on right-side (block black arrow).

Bell's palsy: Bell's Palsy (facial palsy) doesn't require imaging in typical cases. MRI is done in atypical cases like gradual-onset palsy, slowly progressive palsy, facial palsy accompanied by spasm, recurrent palsy, unusual degrees of pain, and the presence of multiple cranial neuropathies or other neurologic symptoms. In post Gad scan, enhancement of facial nerve is most pronounced in the region of the geniculate ganglion, without nodularity. If nodular enhancement is seen, then other causes should be sought [Table/Fig-15] [13].

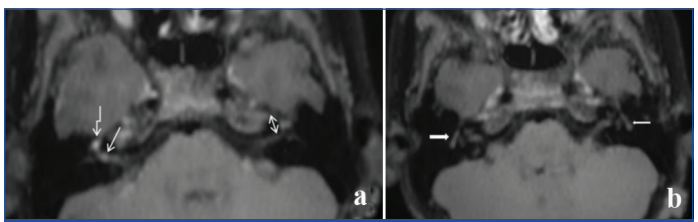

[Table/Fig-15]: Bell's palsy. A 10-year-old male child presented with right-sided facial palsy. Axial reformatted T1 CUBE postcontrast images: (a) Show focal enhancement in intracanalicular part of right facial nerve (white arrow) and labyrinthine segment (curved white arrow). Left intracanalicular part of facial nerve doesn't show increased enhancement (double-headed arrow); (b) Horizontal part of both facial nerves show normal mild increased enhancement (white block arrows).

Demyelination: Demyelinating ON, usually presents with painful loss of vision in young or middle-aged adults. It can present as an isolated or with Multiple Sclerosis (MS) in most of the cases. A 50% patients presenting with isolated ON develop MS later in the course of the disease [14]. Demyelinating ON can present in MS, Neuromyelitis Optica Syndrome Disorder (NMO-SD), Acute Disseminated Encephalomyelitis (ADEM) and anti MOG antibody disease. In NMO-SD ON, intracranial, chiasmal and optic tract involvement is seen while in MOG ON, intraorbital ON involvement is seen with peri optic fat stranding [Table/Fig-16,17] [15]. Optic neuritis is not common in ADEM while MS presents with frequent optic nerve involvement, most commonly intraorbital and intracanalicular segments. In demyelinating ON, the nerve shows increased T2 signals with some degree of enhancement on postcontrast study [15].

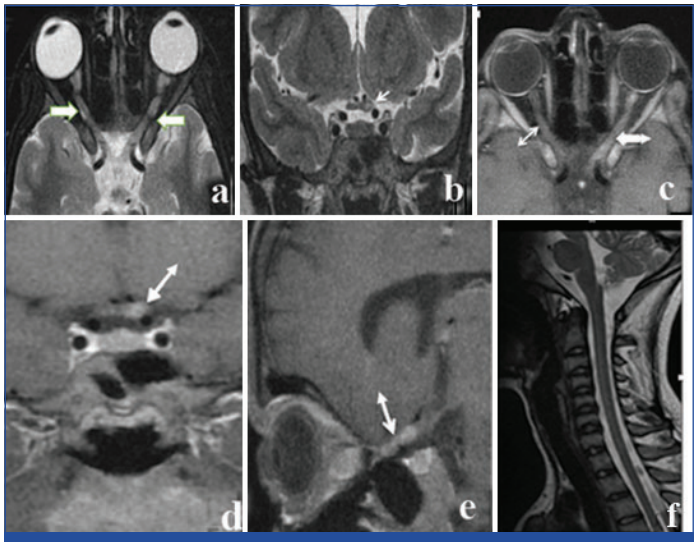

[Table/Fig-16]: Clinically suspected to have bilateral Optic Neuritis (ON). A 20-year-old female presented with bilateral painful loss of vision. (a) Axial (b) Coronal T2 weighted images show hyperintense and thickened intraorbital, canalicular, intracranial segments of both optic nerves (white block arrows) and optic chiasma on left-side (white arrow). (c) Axial (d) Coronal (e) Sagittal postcontrast images show enhancing both optic nerves and optic chiasma on left-side (double-headed arrows). (f) Sagittal T2 weighted image shows normal signal intensity in cervical cord. No altered signal intensity noted in brain (not shown). Patient came to be positive for anti NMO/aquaporin4 antibodies and diagnosed as sero-positive neuromyelitis optica spectrum disorder.

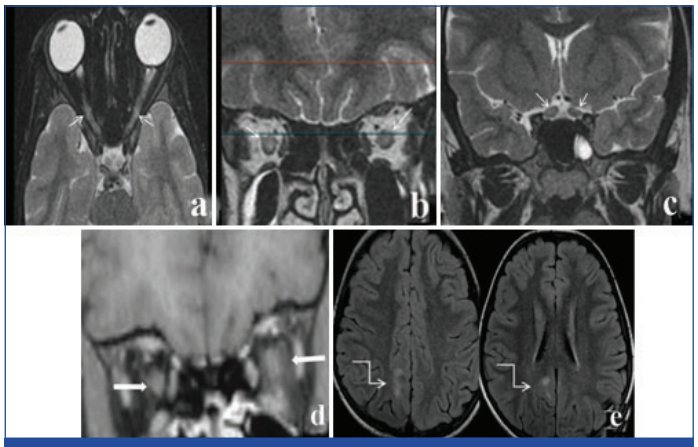

[Table/Fig-17]: A 14-year-old female presented with bilateral painful vision loss. (a) Axial T2 (b,c) T2 weighted images show mildly thickened bilateral optic nerves throughout their course (white arrows) with perioptic orbital fat stranding, more prominent on left-side and showing enhancement (block white arrows) (d). Focal few areas of juxta-cortical and U fibre hyperintensity seen in right posterior parasagittal parietal region on T2 images (curved white arrows) suggesting demyelinating lesions. Corpus callosum appears normal (not shown). No Dawson fingers. Spinal cord screening is also normal (not shown). Patient came positive for anti MOG antibodies and diagnosed to have MGO antibody disorder with bilateral ON with perioptic orbital fat enhancement and demyelinating lesions in brain parenchyma.

Neoplastic: Primary Nerve Tumours-schwannoma is the most common primary CN tumour which can develop in any CN except those which lack schwann cells (I and II). Vestibulocochlear nerve (VIII) is the most commonly involved followed by trigeminal (V), facial (VII), glossopharyngeal (IX), vagus (X), spinal accessory (XI), and hypoglossal (XII) nerves [16]. The CN tumours appear heterogeneously hyperintense on T2 weighted images and showed avid postcontrast enhancement with or without presence of non enhancing cystic/necrotic areas [Table/Fig-18,19]. Other group of tumours includes optic pathway gliomas and esthesioneuroblastoma [Table/Fig-20] [17]. The optic nerve sheath meningioma arises from arachnoid cell layer and not from neural structure, hence not included in the present study.

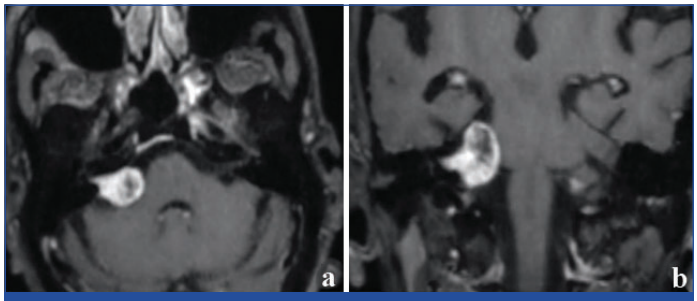

[Table/Fig-18]: Acoustic schwanomma in a 65-year-old male. Postcontrast Axial: (a) Coronal images show; (b) Ice cream cone appearance. Icecream in the CP cistern and cone within the IAC along 7-8th nerve complex.

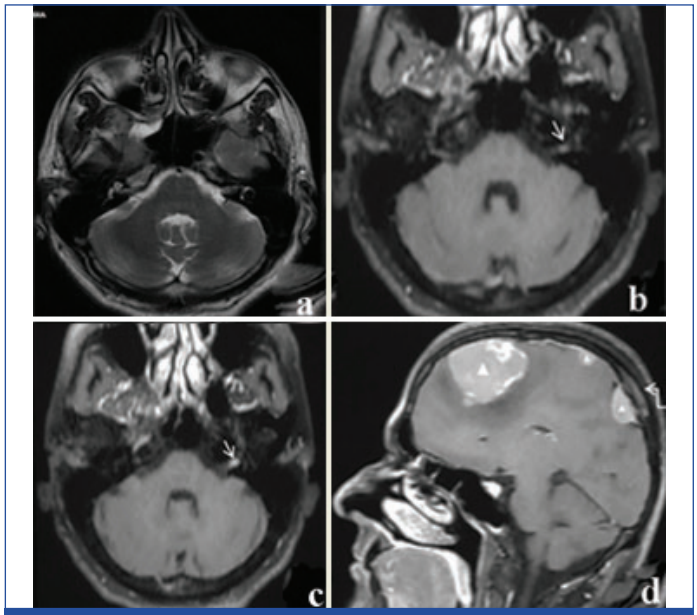

[Table/Fig-19]: Neurofibromatosis 2 in a 38-year-old male. (a) Axial T2 weighted image shows bilateral internal acoustic canals with no obvious abnormality. (b-d) Axial reformatted T1 CUBE postcontrast images image show tiny enhancing left intracanalicular acoustic schwanomma (white arrow) and multiple homogenously enhancing convexity meningiomas (arrow head) and hyperostosis associated with the lesion (curved white arrow).

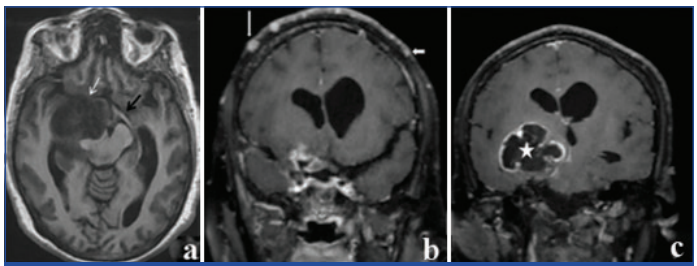

[Table/Fig-20]: A 30-year-old female, known case of Neurofibromatosis 1 (NF1), presented with right-sided vision loss. (a) Axial 3D T1 weighted Brain volume (BRAVO) image lobulated T1 hypointense lesion arising from right optic tract (white arrow), contralateral normal left optic tract (black arrow); (b,c) Coronal reformatted T1 CUBE postcontrast images show multiple enhancing nodular lesions in scalp (neurofibromas) (block white arrows) and peripherally enhancing mass lesion along right optic tract (glioma) (white star).

Malignant nerve tumors-retinoblastoma is a malignant tumour that involves the eyeball and may spread along the optic nerve up to the optic chiasma [Table/Fig-21]. Perineural spread of malignancy can occur in various head and neck malignancies like adenoid cystic carcinoma, squamous cell carcinoma, mucoepidermoid

carcinoma, basal cell carcinoma, rhabdomyosarcoma and other sarcomas [18]. Leptomeningeal spread of tumours can present as multiple CN involvement as seen in primary intraaxial tumours like medulloblastoma, ependymoma, oligodendroglioma, and glioblastoma or secondary tumours (leukaemia/lymphoma, breast, lung, renal and prostate carcinomas and melanoma) [1,8]. Neural involvement can manifest in the form of thickening, irregularity and/or enhancement of the CN and their branches, which is best appreciated in 3D CUBE T1 contrast FS sequence [Table/Fig-22-30]. Also, associated signs like enlargement of cranial neural foramina, obliteration of perineural fat on T1 TSE images, muscle denervation presenting as T2/STIR hyperintensity or fatty infiltration of muscles can be seen [Table/Fig-31] [18,19].

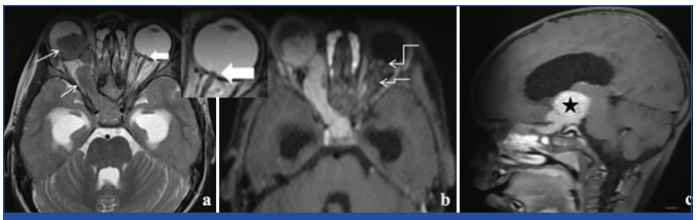

[Table/Fig-21]: Bilateral retinoblastoma. A 5-year-old male presented with bilateral gradual progressive loss of vision and right eye proptosis. (a) Axial T2 weighted image shows mild T2 hyperintense mass lesion in right eyeball in vitreous humour (white arrow) extending along the optic nerve upto the optic chiasma presenting as suprasellar mass. Small lesion also seen in left optic disc (block white arrow), also shown in cropped left eyeball image; (b) Axial (c) Sagittal postcontrast images show homogenous moderate enhancement of the tumour extending upto suprasellar region (black star). Focal enhancing lesion seen at optic nerve head and along left optic nerve (curved white arrows in b).

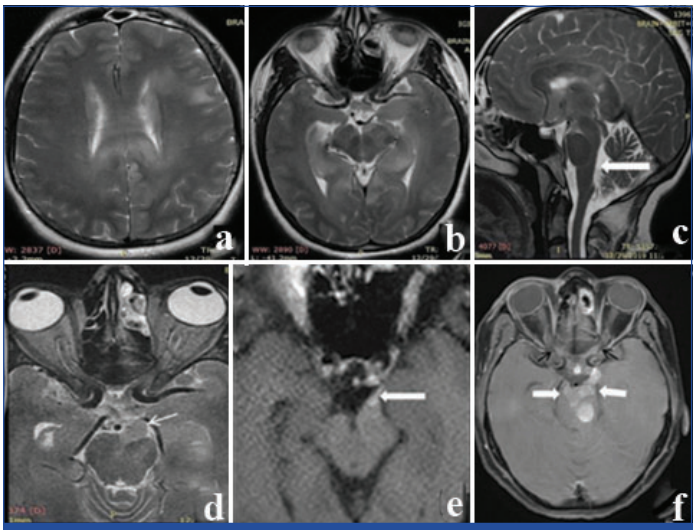

[Table/Fig-22]: Gliomatosis cerebri with high-grade transformation. A 44-year-old female patient with history of ptosis and diplopia since one month back. Axial (a,b) and Sagittal T2 (c), Axial T2FS (d) Hyperintensity in corpus callosum, asymmetrical sub cortical white matter, bilateral thalamus, bilateral hippocampus, midbrain, bulky left third nerve (white arrow). (e) And On 3D cube postcontrast sequence, left oculomotor nerve appears thickened and shows enhancement.(block white arrow). (f) Axial postcontrast image after an interval of two months shows increase in the size of lesion in midbrain, enhancing and thickened both optic (black arrows) and oculomotor nerves (block white arrows).

Tolosa hunt syndrome: Schuknecht B et al., evaluated 15 patients with painful ophthalmoplegia and found enhancing soft tissue with lateral bulging contour of cavernous sinus in all patients. Associated signs were internal carotid artery narrowing, extension to superior orbital fissure and orbital apex and complete resolution of findings with steroid treatment on six months follow-up [20]. In the present study, findings were similar and marked improvement of symptoms was seen after starting of steroids and on follow-up [Table/Fig-32].

Idiopathic polyneuritis cranialis: It is a rare disorder that can affect multiple CN. Torres AR et al., described the disorder in a young male who presented with multiple episodes of different CN palsies. The most common nerves affected are IV, V, VI and VII CNs. Its aetiology is multifaceted such as inflammatory, infective, autoimmune, toxin mediated, vitamin deficiency, granulomatous,

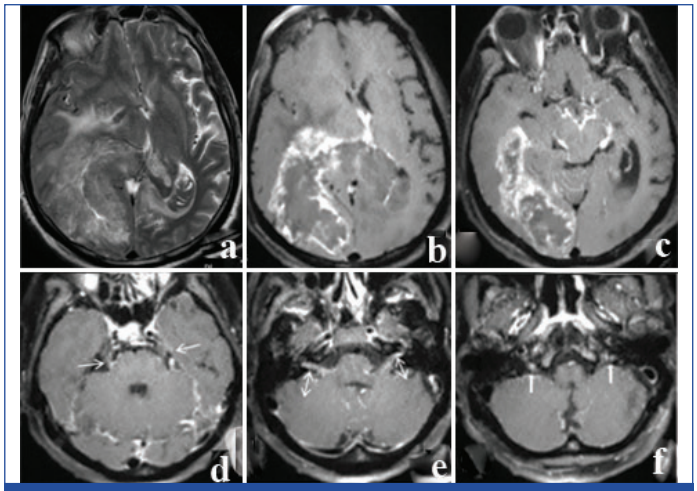

[Table/Fig-23]: Glioblastoma multiforme with leptomeningeal carcinomatosis and neural infiltration. A 67-year-old male presented with altered sensorium: (a) Axial T2 weighted image shows hyperintense lesion in right occipital lobe with intraventricular extension and perilesional oedema causing mass effect; (b-e) Axial reformatted T1 CUBE postcontrast images show peripheral irregular enhancement of the mass lesion seen with intraventricular extension and intraventricular bleed. Patient expired few days after the scan. Bilateral 5th (white arrows in d), 7-8th (double-headed arrows in e) and 9-10-11th (white block arrows in f) Nerve complex enhancement seen.

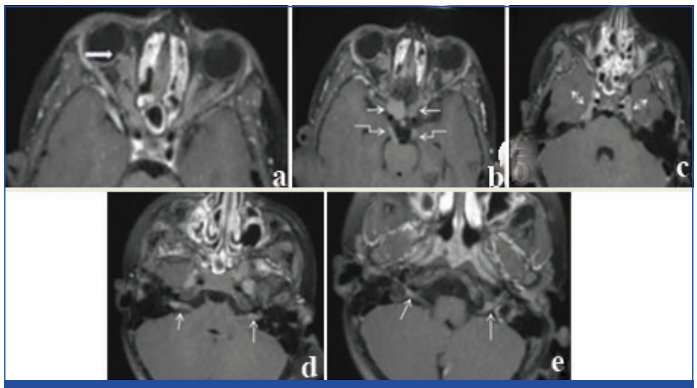

[Table/Fig-24]: K/C/O Acute lymphocytic leukaemia with neural infiltration on treatment- A 6-year-old male presented with loss of vision in both eyes, headache and papilloedema. 3D T1 CUBE FS postcontrast sequence shows (a) Thick enhancing bilateral optic nerves with optic nerve head protrusion (white arrow), (b) Nodular enhancing deposit in intracranial segment of optic nerves (arrow), enhancing and thickened bilateral 3rd (b-curved arrows), 5th (c-double-headed arrows), 7-8th (d-arrows) and 9, 10 and 11th nerve complex (e-arrows).

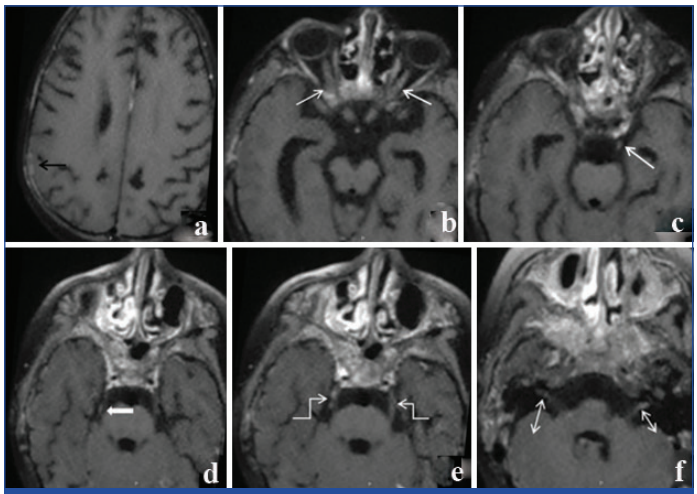

[Table/Fig-25]: ALL with neural infiltration. A 10-year-old male with leukaemia presented with history of status epilepticus, postcontrast T1 Cube axial reformatted image shows micronodular enhancement at right parietal region (black arrow in 'a'), bilateral optic nerve enhancement (white arrows in b), left oculomotor nerve enhancement (white arrow in c), right trochlear nerve enhancement (block white arrow in d), bilateral 5th nerve enhancement (curved white arrow in e), bilateral 7th-8th nerve complex enhancement (double-headed arrow in f).

connective tissue disorders or idiopathic [21]. In the present study, no aetiology was found in work-up [Table/Fig-33]. [Table/Fig-34] summarises all aetiologies of pathological CN enhancement and how to differentiate them.

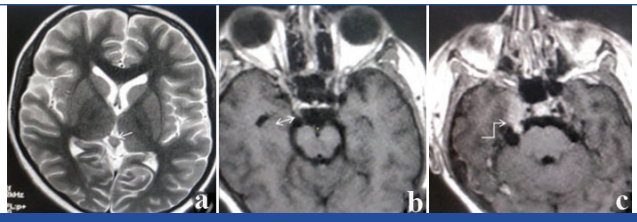

[Table/Fig-26]: A 10-year-old female with Burkitt lymphoma and right oculomotor and right trigeminal nerve palsy. Axial T2 weighted image shows pineal gland lesion (white arrow). Axial reformatted T1 CUBE postcontrast (b,c) Shows right oculomotor nerve (double-headed arrow) and right trigeminal nerve enhancement (curved white arrow) site of infiltration.

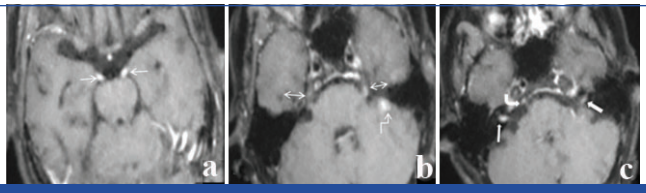

[Table/Fig-27]: Known case of chronic myeloid leukaemia. A 50-year-old male presented with headache, recurrent vomiting, abnormal movement of limbs and constipation. Axial reformatted CUBE T1 axial images (a-c) Shows enhancing bilateral 3rd (white arrows), 5th (double-headed arrows), nodular enhancing deposit in left anterior cerebellum (curved white arrow), enhancing right 6th nerve (block curved arrow) and bilateral intracanalicular segment of 7-8th nerve complex (block white arrows) site of infiltration.

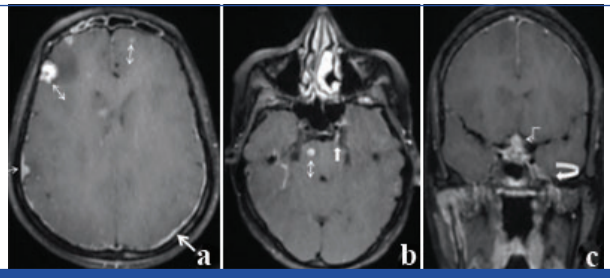

[Table/Fig-28]: Neural infiltration due to metastasis from breast cancer-3D Postcontrast (a,b) Axial reformatted CUBE sequence shows nodular dural enhancement (white arrow), thick ring and nodular enhancing lesions (double-headed arrows), left 5th nerve enhancement in cistern (block white arrow), (c) Coronal reformatted image shows enhancing deposit in suprasellar region (curved thin white arrow) and enhancing V3 segment in foramen ovale (thick curved white arrow).

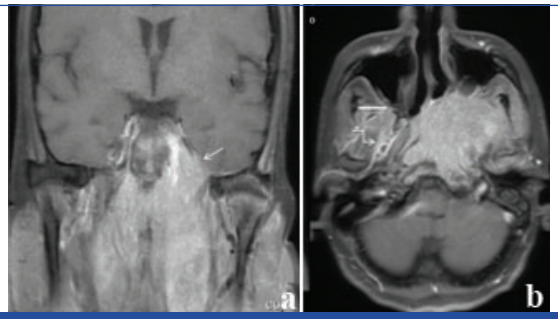

[Table/Fig-29]: Nasopharyngeal carcinoma involving V2 and V3 branch of trigeminal nerve. (a) Postcontrast coronal reformatted T1 CUBE sequence shows thick enhancing V3 branch (white arrow), (b) Axial reformatted image shows normal pterygopalatine fossa (block white arrow) and mandibular nerve (V3) below foramen ovale (curved white arrow) on right-side. Both nerves are involved on left-side.

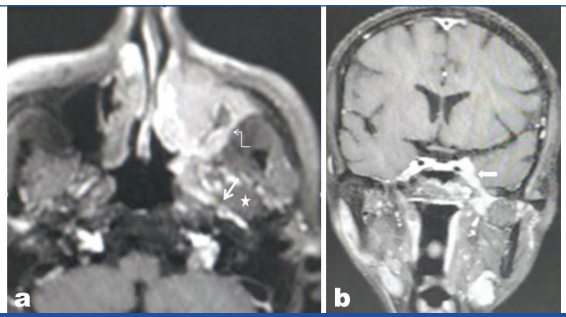

[Table/Fig-30]: Maxillary carcinoma with V3 perineural infiltration. (a) Axial reformatted T1 CUBE postcontrast image shows enhancing soft tissue involving left maxillary sinus and retroantral space (curved white arrow), enhancing V3 branches (white arrow) medial to lateral pterygoid muscle (star), (b) Coronal reformatted image shows infiltration extend upwards through foramen ovale into Meckel's cave (block white arrow).

Cranial nerve (or branch)	Important Space(s)/foramina
Ophthalmic division of trigeminal nerve (V1)	Supraorbital foramen
Maxillary division of trigeminal nerve (V2)	Foramen rotundum, the pterygopalatine fossa, the canal and foramen for the infraorbital nerve, the vidian canal, and the palatine foramen
Mandibular division of trigeminal nerve (V3)	Foramen ovale and the mandibular foramen for the inferior alveolar nerve
Facial nerve	Stylomastoid foramen and descending facial nerve canal

[Table/Fig-31]: The following are the areas to be seen when perineural spread is suspected [18].

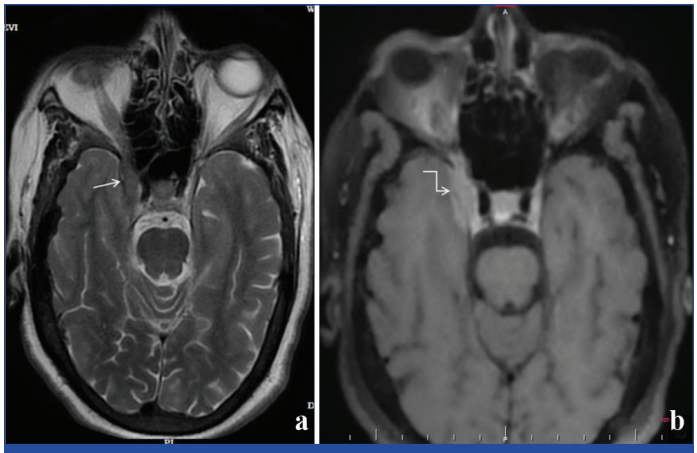

[Table/Fig-32]: Tolosa hunt syndrome. A 62-year-old female presented with right 3rd Cranial Nerve (CN) palsy. (a) Axial T2 weighted image shows iso to hypointense lesion in cavernous sinus extending upto the orbital apex (white arrow) and (b) Postcontrast axial reformatted T1 CUBE image shows moderate soft tissue enhancement (curved white arrow). There was marked improvement of symptoms when steroids were started.

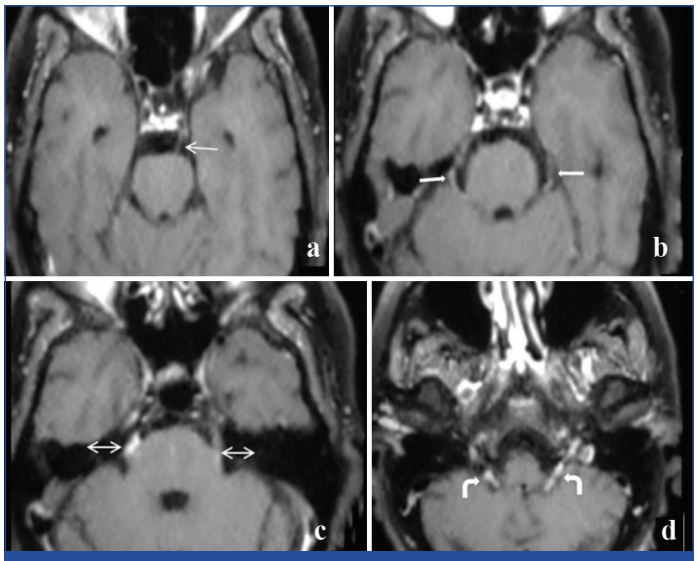

[Table/Fig-33]: Idiopathic polyneuritis cranialis. History of recurrent Cranial Nerve (CN) palsy, first episode 20 years back, now presented with left facial paresthesia. (a-d) Postcontrast axial reformatted T1 CUBE images show mild enhancement involving left 3rd (white arrow in a), bilateral 4th (white arrows in b), bilateral 5th (right>left, (double-headed arrows) in c) and bilateral 9-10-11th nerve complex (curved white arrows in d). Differentials include granulomatous disorder (sarcoidosis), neuro-lymes disease, lymphoproliferative disorder, immune mediated, ophthalmoplegic migraine or idiopathic polyneuritis cranialis.

CNS tuberculosis	Strong clinical suspicion, basal cistern exudates and leptomeningeal enhancement, presence of conglomerated T2 hypointense ring enhancing lesions, multiple CN/perineural sheath enhancement
Fungal disease	Usually, associated sinus disease which appears T1 hyperintense and T2 hypointense, may present with orbital apex syndrome or involvement of cavernous sinus, may have dural enhancement or fungal abscess
Herpes zoster ophthalmicus	Presence of unilateral facial pain and vesicles (clinical history) with optic nerve, cavernous sinus or trigeminal nerve enhancement
Viral neuritis and labyrinthitis	Presence of acute vertigo or hearing loss with nausea and associated nerve enhancement

Demyelination	Presence of ON with history of sudden painful diminution of vision. May have T2/FLAIR white matter or spinal cord hyperintensities, perioptic fat stranding in MOG-ON, chiasmal and optic tract involvement is more common in NMOSD-ON, confirmation by CSF examination and presence of antibodies seen in NMO-SD/anti MOG, oligoclonal bands in Multiple Sclerosis (MS)
Lyme's disease	Transmitted by borrelia tick, causes focal lesions in white matter of brain, nerve root or meningeal enhancement. May affect other organ systems
Sarcoidosis	Most patients with neurosarcoidosis at presentation have extracranial manifestations, CN enhancement (VII-VIII, I, II), pachymeningeal enhancement, sarcoid granulomas in brain parenchyma
Primary nerve tumour	Typical appearance in cases of acoustic schwannoma (ice cream cone appearance), trigeminal schwannoma (dumb-bell shape), optic nerve glioma (mass like thickening of optic nerve or tract, may be associated with NF1)
Malignant primary nerve tumour	Esthesioneuroblastoma (mass in upper half of nasal cavity with involvement of base of skull, olfactory fossa, presence of cystic component in cranial aspect)
Nerve infiltration by primary brain malignancy	Imaging findings of primary brain malignancy, meningeal carcinomatosis can lead to nerve infiltration
Haematological malignancy (ALL, CLL, Burkitt's lymphoma)	Clinical history of primary haematological malignancy along with bone marrow findings, systemic symptoms and other organ involvement, nodular enhancing neural thickening, may have dural enhancement and parenchymal deposits
Brain metastasis with neural infiltration (breast cancer)	History of primary malignancy, nodular or irregular ring enhancing brain parenchymal lesions with extensive surrounding oedema, dural deposits, multiple lesions, nodular or smooth thickening of nerves with enhancement
Perineural spread of tumour (from nasopharyngeal Ca, oropharyngeal Ca, maxillary Ca)	Presence of primary malignancy, obscuration of perineural fat compared to opposite side on T1 weighted images, enhancement along the nerves with secondary signs (refer to [Table/Fig-2])
Tolosa hunt syndrome	T1/T2 hypointense soft tissue in anterior cavernous sinus, enhancement in postcontrast study, associated signs of internal carotid artery narrowing, orbital apex extension and resolution on steroid treatment

[Table/Fig-34]: Shows the differentiating points to distinguish various diseases showing nerve enhancement.

Limitation(s)

The limitations of the study include small sample size diseases like neurosarcoidosis atypical infections affecting the CN were not included in the study.

CONCLUSION(S)

Presence of nerve enhancement is a strong predictor of underlying pathology and may be the only sign of disease in MRI brain studies. Clinical history with other associated findings on imaging help in reaching the final diagnosis. A 3D CUBE T1 sequence helps in picking up even subtle nerve enhancements, hence, should always be a part of brain MRI imaging.

REFERENCES

[1] Krainik A, Casselman JW. Imaging Evaluation of Patients with Cranial Nerve Disorders. 2020 Feb 15. In: Hodler J, Kubik-Huch RA, von Schulthess GK, editors. Diseases of the Brain, Head and Neck, Spine 2020-2023: Diagnostic Imaging [Internet]. Cham (CH): Springer; 2020. Chapter 12. PMID: 32119250.
[2] Saremi F, Helmy M, Farzin S, Zee CS, Go JL. MRI of cranial nerve enhancement. Am J Roentgenol. 2005;185(6):1487-97.
[3] Majigsuren M, Abe T, Kageji T, Matsuzaki K, Takeuchi M, Iwamoto S, et al. Comparison of brain tumour contrast-enhancement on t1-cube and 3d-spgr images. Magn Reson Med Sci. 2016;15(1):34-40.
[4] Hasegawa H, Ashikaga R, Okajima K, Wakayama T, Miyoshi M, Nishimura Y, et al. Comparison of lesion enhancement between BB Cube and 3D-SPGR images for brain tumours with 1.5-T magnetic resonance imaging. Jpn J Radiol. 2017;35(8):463-71.
[5] Park YW, Ahn SJ. Comparison of contrast-enhanced T2 FLAIR and 3D T1 black-blood fast spin-echo for detection of leptomeningeal metastases. Investig Magn Reson Imaging. 2018;22(2):86.
[6] Yamaguchi K, Takahashi S, Hosoya T, Nagahata M, Yamaguchi K. Abducens neuropathy detected by three-dimensional magnetic resonance imaging using a multiplanar reconstruction technique with gadolinium-DTPA enhancement. Jpn J Ophthalmol. 1997;41(1):59-61.
[7] Tanenbaum LN. Contrast-enhanced neuro MRI: Issues and indications. Appl Radiol. 2015;(May):01-04.
[8] Romano N, Federici M, Castaldi A. Imaging of cranial nerves: A pictorial overview. Insights Imaging. 2019;10:33. https://doi.org/10.1186/s13244-019-0719-5.
[9] Misra UK, Kalita J, Bhoi SK. Spectrum and outcome predictors of central nervous system infections in a neurological critical care unit in India: A retrospective review. Trans R Soc Trop Med Hyg. 2014;108(3):141-46.
[10] Garg RK, Malhotra HS, Jain A. Neuroimaging in tuberculous meningitis. Neurol India. 2016;64(2):219-27.
[11] Li X, Ma L, Zhang L, Wu X, Chen H, Gao M. Clinical characteristics of tuberculous meningitis combined with cranial nerve palsy. Clin Neurol Neurosurg. 2019;184:105443.
[12] Gavito-Higuera J, Mullins C, Ramos-Duran L, Olivas Chacon C, Hakim N, Palacios E. Fungal infections of the central nervous system: A pictorial review. J Clin Imaging Sci. 2016;6(2):01-06.
[13] Lanser MJ, Jackler RK. Gadolinium magnetic resonance imaging in Bell's palsy. West J Med. 1991;154(6):718-19.
[14] Voss E, Raab P, Trebst C, Stangel M. Clinical approach to optic neuritis: Pitfalls, red flags and differential diagnosis. Ther Adv Neurol Disord. 2011;4(2):123-34.
[15] Weber MS, Derfuss T, Metz I, Brück W. Defining distinct features of anti-MOG antibody associated central nervous system demyelination. Ther Adv Neurol Disord. 2018;11:175628641876208.
[16] Skolnik AD, Loevner LA, Sampathu DM, Newman JG, Lee JY, Bagley LJ, et al. Cranial nerve schwannomas: Diagnostic imaging approach. Radiographics. 2016;36(5):1463-77.
[17] Wowra B. TJ. Oncology of CNS tumours. In: Tonn JC, Westphal M. RJT, editor. Oncology of CNS Tumours. Second. Springer, Berlin, Heidelberg; 2010. Pp. 251-67.
[18] Gandhi D, Gujar S, Mukherji SK. Magnetic resonance imaging of perineural spread of head and neck malignancies. Top Magn Reson Imaging. 2004;15(2):79-85.
[19] Chong V. Imaging the cranial nerves in cancer. Cancer Imaging. 2004;4:S01-05.
[20] Schuknecht B, Sturm V, Huisman TAGM, Landau K. Tolosa-Hunt syndrome: MR imaging features in 15 patients with 20 episodes of painful ophthalmoplegia. Eur J Radiol. 2009;69(3):445-53.
[21] Torres AR, Salvador C, Mora M, Mirchandani S, Chavez W. Idiopathic recurrent polyneuritis cranialis: A rare entity. Cureus 2019;11(4):e4488. Doi: 10.7759/cureus.4488.

PARTICULARS OF CONTRIBUTORS:
1. Assistant Professor, Department of Radiodiagnosis, IGIMS, Patna, Bihar, India.
2. Senior Resident, Department of Radiodiagnosis, IGIMS, Patna, Bihar, India.
3. Assistant Professor, Department of Radiodiagnosis, IGIMS, Patna, Bihar, India.
4. Professor, Department of Radiodiagnosis, IGIMS, Patna, Bihar, India.
5. Assistant Professor, Department of Radiodiagnosis, IGIMS, Patna, Bihar, India.

NAME, ADDRESS, E-MAIL ID OF THE CORRESPONDING AUTHOR:
Ruchi Gupta,
Assistant Professor, Department of Radiodiagnosis, IGIMS, Patna, Bihar, India.
E-mail: drruchigupta28@gmail.com

PLAGIARISM CHECKING METHODS: [Jain H et al.]
- Plagiarism X-checker: Jul 01, 2022
- Manual Googling: Feb 08, 2023
- iThenticate Software: Mar 28, 2023 (5%)

ETYMOLOGY: Author Origin

AUTHOR DECLARATION:
- Financial or Other Competing Interests: None
- Was Ethics Committee Approval obtained for this study? Yes
- Was informed consent obtained from the subjects involved in the study? Yes
- For any images presented appropriate consent has been obtained from the subjects. Yes

Date of Submission: **Jun 30, 2022**
Date of Peer Review: **Oct 05, 2022**
Date of Acceptance: **Mar 29, 2023**
Date of Publishing: **Jun 01, 2023**